Available online at www.sciencedirect.com
ScienceDirect
Fluid Phase Equilibria 250 (2006) 116–124
FLUID PHASE EQUILIBRIA
www.elsevier.com/locate/fluid

Carbon dioxide, ethylene and water vapor sorption in poly(lactic acid)

N.S. Oliveira [a], C.M. Gonçalves [a], J.A.P. Coutinho [a], A. Ferreira [b], J. Dorgan [c], I.M. Marrucho [a,*]

[a] *CICECO, Departamento de Química, Universidade de Aveiro, 3810-193 Aveiro, Portugal*
[b] *CICECO, ESTGA, Ap. 473, 3754-909 Águeda, Portugal*
[c] *Colorado School of Mines, Golden, CO 80401, USA*

Received 19 July 2006; received in revised form 28 September 2006; accepted 15 October 2006
Available online 21 October 2006

Abstract

The objective of this work is to study the gas/vapor sorption in poly(lactic acid) (PLA) with a 98:2 (L:D) ratio using a quartz crystal microbalance (QCM). For that purpose, the sorption of carbon dioxide, ethylene and water vapor in poly(lactic acid) (PLA) with a 98:2 (L:D) ratio, in temperature range from 283 to 313 K and up to atmospheric pressure was measured. The measured isotherms indicate that the sorption mechanism is sorbate dependent, since carbon dioxide and ethylene seem to have predominantly a Langmuir type of mechanism while water is predominantly Henry controlled. Two temperature protocols were used and only ethylene sorption is affected by them. Comparisons with previously measured gas sorption data in PLA 80:20 using the same temperature protocol indicate that the L:D ratio plays a dominant role in gas/vapor sorption in PLA.

Keywords: Sorption; Biodegradable polymer; Quartz crystal microbalance; Poly(lactic acid) (PLA)

1. Introduction

The need for the development of new materials based on renewable sources has led to the development of new polymers, such as the polylactide polymers (PLA). PLA have been used since 1970s for biomedical and pharmaceutical applications, but the recent development of technology for large scale fabrication made PLA available at low cost, enabling its use in innumerous other applications. In addition to being thermoplastic, biodegradable, compostable and produced from annually renewable feedstock, PLA shows mechanical and barrier properties similar to synthetic polymers that have been long used for food packaging, like polystyrene (PS) and polyethylene terephthalate (PET) [1].

Due to the chiral nature of lactic acid, the stereochemistry of PLA is complex. The lactides, used as monomers in the production process of PLA, are formed by condensation of two lactic acid molecules. Thus, three types of lactides can be obtained: DD-lactide, LD-lactide and LL-lactide. The chemical formulae of the lactic acid as well as of the lactides are presented in Fig. 1. The control of the L:D ratio of the monomers is an important molecular feature that has large impact on the material properties through its effect on crystallization. The PLA polymers containing more than 93% of L-lactic acid are semi crystalline, while PLA polymers with 50–93% of L-lactic acid are strictly amorphous. The presence of LD- and DD-lactides introduces sufficient irregularity to limit crystallinity. The glass transition temperature (T_g) and the melting temperatures (T_m) are other properties that are also affected by the proportions of the different lactides. For example, the glass transitions temperature of PLA can vary from 323 to 353 K and the T_m ranges from 403 up to 453 K, for different proportions of the LD- and DD-lactides [1,2].

It is well known that the structure of glassy polymers depends upon their thermal history, that is, the local structure of a glassy material is expected to change according to various conditions of the glass formation. Sub-T_g annealing, thermal quenching, CO_2 or He pressure conditioning are the most used physical treatments applied to glassy polymers in general to study a specific system for a specific application. Several authors used the quartz crystal microbalance to study the influence of the thermal history of the polymer in the gas sorption [3–7] and concluded that for casted films, the slower the thermal conditioning is applied

* Corresponding author. Tel.: +351 234 401 406; fax: +351 234 370 084.
E-mail address: IMARRUCHO@DQ.UA.PT (I.M. Marrucho).

0378-3812/$ – see front matter © 2006 Elsevier B.V. All rights reserved.
doi:10.1016/j.fluid.2006.10.009

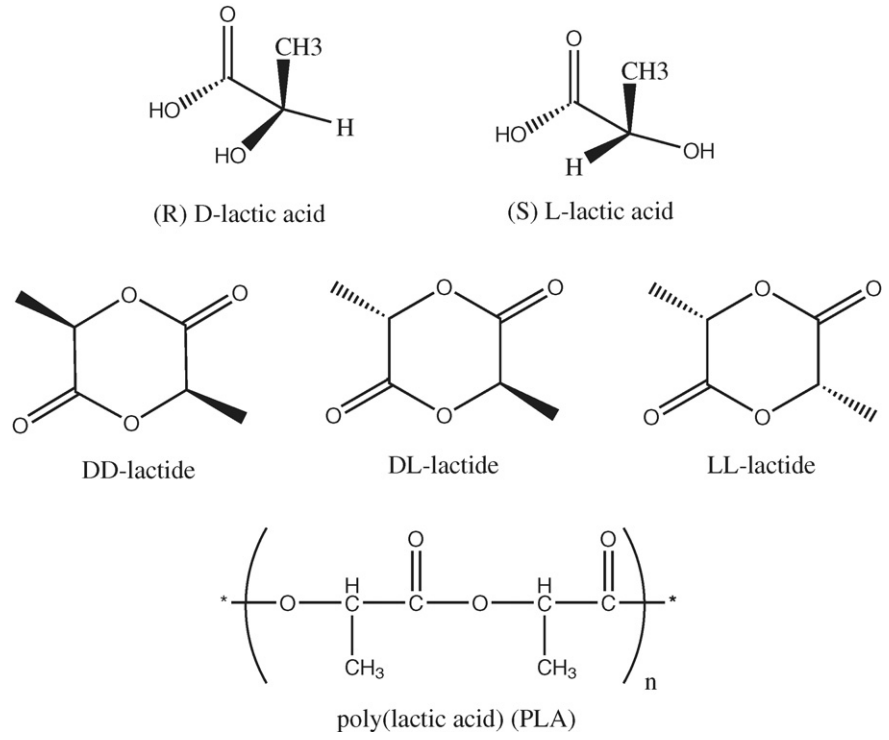

Fig. 1. Chemical structure of PLA and its constituents.

the more complete the relaxation of the casted glassy polymer film, diminishing the excess free volume available for sorption. Oliveira et al. [6,7] performed sorption studies of carbon dioxide in PLA using the quartz crystal microbalance and three different thermal protocols and concluded that the polymer film thermal history only has significant impact in gas sorption for pressures higher than 2 MPa (Fig. 2).

This work aims at studying the sorption of gases, namely CO_2, C_2H_4 and water vapor in PLA 98:2 (L:D) in the temperature range from 283 to 313 K and pressures up to the atmospheric pressure, using a quartz crystal microbalance. The major advantage of this method is the short time required to reach equilibrium, which in this case ranges from 3 to 15 min, while retaining good accuracy and precision. In order to con-

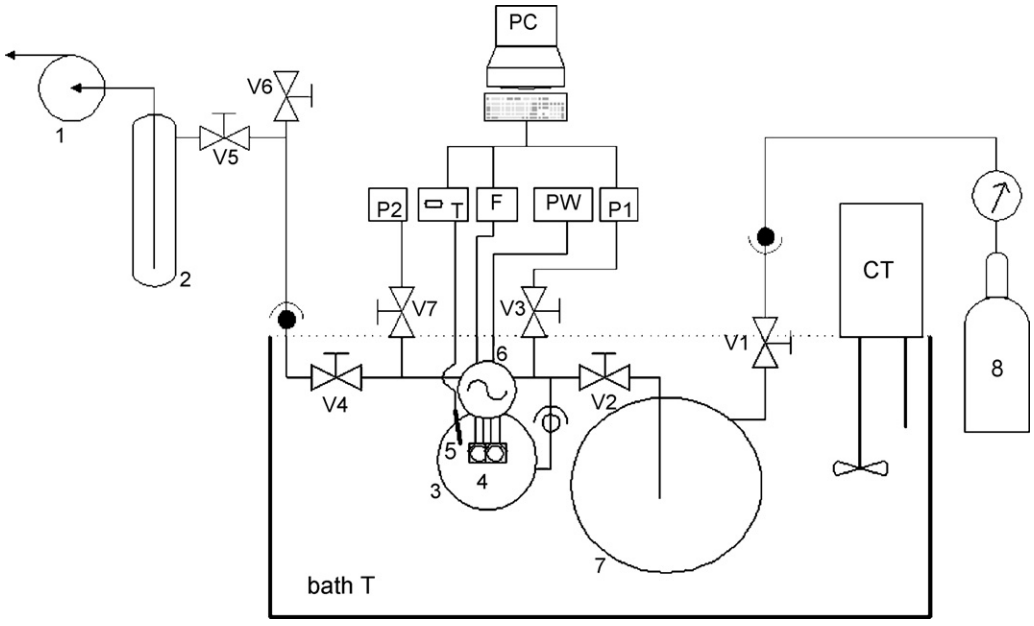

Fig. 2. The QCM apparatus. (1) Vacuum pump; (2) nitrogen trapp; (3) solubility cell; (4) quartz crystals; (5) Pt100 thermometer; (6) double oscillator; (7) gas/vapor thermostat; (8) gas bottle; CT: temperature controller; P1: pressure sensor for gases; PW: oscillator power supply; F: frequency counter; T: multimeter; P2: pressure sensor for vapors; PC: computer; V1–V7: valves.

firm that the thermal treatment of the PLA 98:2 polymer film has little effect in the CO_2, C_2H_4 and water vapor sorption, at the temperature and pressure conditions of this work, the sorption of these gases with two different thermal protocols were also experimentally determined.

2. Experimental

2.1. Materials

Linear poly(lactic acid) (M_w 87,131 Da) with (L:D) ratio of 98:2 was provided by Cargill–Dow polymers in the form of pellets. Carbon dioxide with 99.999% mol/mol minimum stated purity was purchased from air liquide. Dichloromethane was obtained from Riedel–deHaan with analytical reagent grade. Ethylene was purchased from Aldrich with 99.5% of purity. Solvent and gases were used with no further purification. The quartz crystals were of 9 MHz base frequency, with golden electrodes of 5 mm and were supplied by Euroquartz, England and by ICM, USA.

A Differential Scanning Calorimeter, DSC-50/DTA-50 from Shimadzu, was used to measure the glass transition temperature and the melting temperature of PLA (98:2). The crystallinity of the polymer films was estimated with X-ray diffraction tests performed in a Philips X'Pert automatic X-ray diffractometer with 2θ from 5° and 30°.

2.2. Method

The scheme of the QCM apparatus used in this work is presented in Fig. 2. This apparatus operates in the pressure range from 2×10^{-6} to 1 bar and in the temperature range from 263 to 340 K. Since it was described in detail by Oliveira et al. [8], only a brief overview is given here. The solubility cell, which has a volume of 100 cm^3 approximately, and the gas/vapor thermostat are placed inside of a large water bath, capable of maintaining the temperature to within 0.1 K. Two AT-cut quartz crystal of 9 MHz, the reference and the measuring crystals, were mounted in the electrical oscillator circuit, inside the solubility cell. The oscillator is powered by a stabilized potential of 5.0 V and both the quartz crystal frequencies were measured using a 10 digits frequency counter Agilent 53131A, from Hewlett Packard. The temperature inside of the solubility cell is monitored with a previously calibrated Pt100 thermometer connected to a 6.5 digital multimeter Agilent 34401A from Hewlett Packard with a precision of 0.1 K. A rotatory high vacuum pump RV3 from BOC Edwards, capable of reaching a vacuum of 0.08 mbar was used. The gas pressure was measured with an AEP transducer Bit02 of four digits and a resolution of 1 mbar, which has a SIT calibration certificate. The water vapor was measured with a pressure sensor CTR91 from Leybold Vakuum with a precision of 0.01 mbar. This pressure sensor was calibrated against a reference, which is traceable to the German national standard at the "Physikalisch-Technische Bundesanstalt (PTB)" in Berlin.

The experiment starts by evacuating the entire apparatus for 2 days. The gas is inserted from the gas bottle into the gas/vapor thermostat and when the desired temperature is attained it is let into the solubility cell, promoting a change in the frequency of both crystals. This frequency change is recorded as a function of time. When a stable frequency is reached, within an acceptable tolerance (less than 1 Hz in 10 min), the reading is accepted and recorded as the equilibrium frequency. The gas is then evacuated from the solubility cell and desorption process takes place.

2.3. Quartz crystal coating

The 9 MHz crystals were thoroughly cleaned with dichloromethane until the base frequency became constant (±2 Hz). A dilute solution of PLA in dichloromethane, about 1% (w/w) was prepared. A thin polymer coating is prepared by dropping this solution on both sides of the quartz crystal electrode surface. The solvent is left to evaporate at ambient conditions and it is considered that all the solvent was evaporated when periodic frequency checks of the coated crystal give a constant result. The total mass of polymer coated on the quartz crystal can be determined by the difference in the oscillation frequency measured before and after coating. To study the effect of the thermal history of the PLA film, two distinct treatments were performed: *the melting treatment*, which consists in heating up the crystal from ambient temperature up to 523 K, at 2 K/min and cool it down to ambient temperature at 10 K/min, and *the annealing treatment*, in which the crystal is introduced in an oven at 336 K, slightly above the glassy transition temperature, for 2 days, cooled at ambient temperature for 1 day and introduced again in the oven at 336 K for 1 day more.

2.4. Mass measurements using QCM

The sorption measurements were performed with a QCM apparatus that is based on the piezoelectric effect observed in an AT-cut quartz crystal. In this work, two quartz crystals were used: a measuring crystal coated with a thin layer of the polymer under study and an uncoated crystal, which is used as reference. If the polymer film is uniformly spread and vibrates synchronously with the quartz crystal, the frequency of the wave is a function of the coated mass. According to the Sauerbrey equation [9], the frequency change of the crystal, ΔF, can be related to a mass change, Δm, by:

$$\Delta F = -k\Delta \mathrm{m} \tag{1}$$

where k is a proportionality constant that includes physical and geometrical properties of the crystal. When gas, or solvent, is injected into the system, the frequencies of both crystals change. This frequency change, ΔF_E, is a sum of three independent terms, hydrostatic ΔF_P, impedance ΔF_V, and sorption ΔF_S [10]:

$$\Delta F_E = \Delta F_S + \Delta F_P + \Delta F_V \tag{2}$$

ΔF_P is proportional to the pressure, while ΔF_V is a function of the properties of the gas (viscosity and density) and of the crystal (base frequency, thickness and density). These two terms, ΔF_P and ΔF_V, were measured together using the reference crystal. For each temperature and pressure, the frequencies of the coated

and the uncoated crystal were experimentally measured and their difference is proportional to the mass of the coating, polymer and gas sorbed in it. Thus, the solubility of the gas in polymer, C, was calculated according to the following equation:

$$C = \frac{\Delta F_S \rho_{pol.} V_m}{\Delta F_C M} \quad (3)$$

where $\rho_{pol.}$ is the polymer density, ΔF_C the difference between the frequencies of the coated and the uncoated crystals after the equilibrium was reached, M the gas molecular weight and V_m is the gas molar volume at STP conditions (22,414 $cm^3\ mol^{-1}$).

3. Dual-mode sorption model

Several models have been used to correlate gas-polymer phase equilibria data. Among them, the Flory–Huggins, the Sanchez–Lacombe equation and the dual mode sorption model are the most used ones. Also worthwhile mentioning is the recent advance of the SAFT family of equations of state in modelling polymer phase equilibria. In the present case, the dual mode sorption model was chosen since it was showed that it provides the most accurate representation of the gas solubility data in PLA [11]. It also allows an interesting interpretation in terms of the two different types of sorption and discussion of the excess free volume in glassy polymers.

This model has been extensively used to model the gas solubilities in glassy polymers and recently reviewed [11]. It assumes that two types of sorption mechanisms take place when a fluid interacts with a glassy polymer: one is Henry's law dissolution in an equilibrium region, a liquid state part, and the other is Langmuir type of sorption in a non-equilibrium region, a solid state part, which accounts for the solute molecules trapped in microcavities. These two types of sorption are typically assumed to occur in non-equilibrium glassy polymers consisting of two parts, a liquid-like, where sorption described by the Henry's law behaviour takes place, and a solid-like, with the Langmuir type of sorption in porous materials. The dual-mode sorption model is described by:

$$C = k_D p + C'_H \frac{bp}{1 + bp} \quad (4)$$

where C is the total concentration of the gas in the polymer film, the gas solubility, k_D the Henry's law coefficient, b represents the hole affinity parameter, which is a measure of the affinity between the solute molecules and the Langmuir sites, C'_H the capacity parameter, characterizing the saturation of these cavities and p is the pressure.

4. Results

4.1. Film characterization

The PLA films were characterized with DSC and X-ray diffraction. All the measurements in DSC were performed up to 473.2 K at 2 K/min with two complete scans. The first scan is used to measure the crystallization percentage, considering 93.6 J/g for a 100% crystalline L-PLA [12] and the second scan is used to calculate the glass transition temperature without polymer stress. The DSC results of the PLA 98:2 films with the two above described thermal treatments are presented in Table 1 and compared with literature results. It can be seen that the thermal treatment does not significantly influence T_g and T_m but it strongly influences the percentage of crystallinity, which is reduced to half when the melted treatment is performed. There is a significant difference between these results and literature results by Auras et al. [1], but no conclusions can be drawn since the thermal treatment performed is not specified.

Table 1
DSC results for the annealed and melted PLA 98:2 films and literature comparisons

	T_g (K)	T_c (K)	T_m (K)	χ (%, v/v)
Annealed	323.5	369.4	435.3	20
Melted	326.0	372.3	439.5	10
Auras et al. [1]	344.6	–	436.6	40

T_g: glass transition temperature, T_c: crystallization temperature, T_m: melting temperature, χ%: percentage of crystallinity.

The results obtained for both films by X-ray diffraction were performed at ambient temperature with 2θ between 5° and 30°, 3 s per step and 0.05°-step width. The crystalline peaks were obtained at 16.6° and 18.7°. The results for PLA 98:2 films obtained by the X-ray diffraction confirm that the crystallization level is about 20% and 10% (v/v) for the annealed and the melted treatment respectively, confirming the results obtained by DSC.

4.2. Sorption results and discussion

In Tables 2–5 and Figs. 3–5 the experimental sorption results for CO_2, C_2H_4 and water vapor in melted PLA 98:2 between 283 and 313 K up to the atmospheric pressure, as well as their correlation with dual-mode sorption model are presented, respectively. The sorption results obtained in this work have a precision of ±0.02 cm^3 (STP) of gas/vapor per cm^3 of polymer. These results were corrected for 100% amorphous polymer, taking into account that the crystalline regions do not accommodate

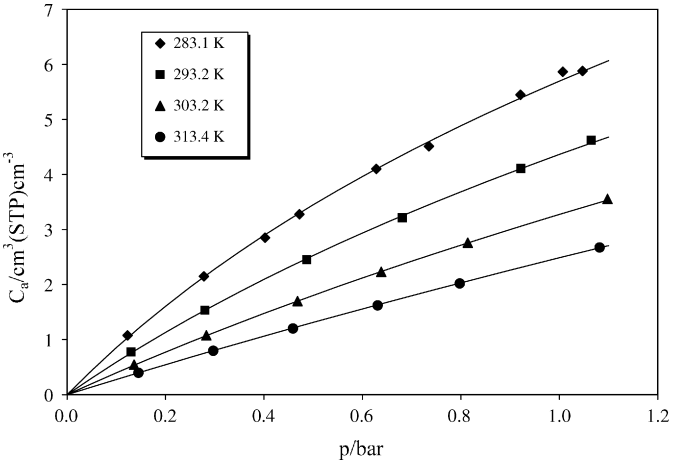

Fig. 3. Sorption isotherms of carbon dioxide in melted PLA 98:2. Continuous lines represent the correlation with dual-mode sorption model.

Table 2
Sorption of carbon dioxide in melted PLA 98:2

T (K)	p (bar)	C (cm^3 (STP) cm^{-3})	C_a (cm^3 (STP) cm^{-3})
283.1	0.123	0.98	1.08
	0.278	1.95	2.15
	0.402	2.59	2.85
	0.472	2.98	3.28
	0.628	3.73	4.10
	0.735	4.10	4.51
	0.921	4.95	5.45
	1.007	5.33	5.86
	1.047	5.34	5.88
293.2	0.130	0.71	0.78
	0.280	1.39	1.53
	0.487	2.23	2.45
	0.681	2.92	3.21
	0.922	3.73	4.11
	1.065	4.20	4.62
303.2	0.136	0.49	0.54
	0.283	0.98	1.08
	0.468	1.54	1.70
	0.638	2.03	2.23
	0.814	2.51	2.76
	1.098	3.23	3.56
313.4	0.145	0.36	0.40
	0.297	0.72	0.79
	0.459	1.09	1.20
	0.631	1.47	1.62
	0.798	1.84	2.02
	1.082	2.43	2.67

Table 3
Critical temperature of the sorbates used in this work [15]

	T_c (K)	V_w ($cm^3\ mol^{-1}$)
CO_2	304.2	22.98
C_2H_4	282.4	24.40
H_2O	647.3	10.45

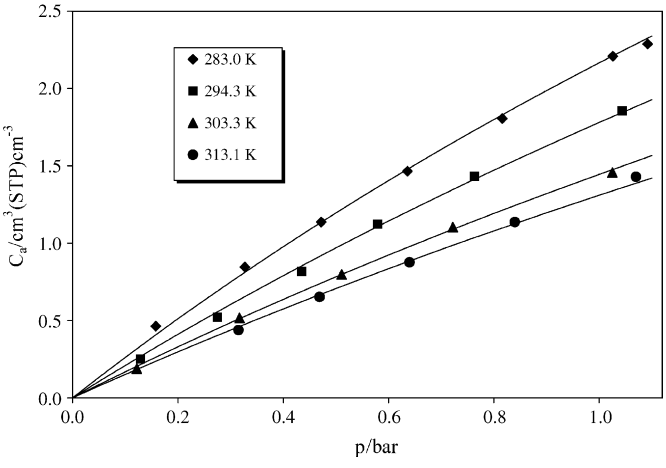

Fig. 4. Sorption isotherms of ethylene in melted PLA 98:2. Continuous lines represent the correlation with dual-mode sorption model.

Table 4
Sorption of ethylene in melted PLA 98:2

T (K)	p (bar)	C (cm^3 (STP) cm^{-3})	C_a (cm^3 (STP) cm^{-3})
283.0	0.158	0.42	0.46
	0.327	0.77	0.85
	0.472	1.03	1.14
	0.636	1.33	1.47
	0.816	1.64	1.81
	1.026	2.01	2.21
	1.092	2.08	2.29
294.3	0.129	0.23	0.25
	0.275	0.47	0.52
	0.435	0.74	0.82
	0.579	1.02	1.12
	0.763	1.30	1.43
	1.044	1.69	1.85
303.3	0.122	0.17	0.19
	0.317	0.47	0.52
	0.511	0.73	0.80
	0.722	1.00	1.10
	1.025	1.32	1.46
313.1	0.315	0.40	0.44
	0.469	0.59	0.65
	0.640	0.80	0.88
	0.840	1.03	1.14
	1.070	1.30	1.43

Table 5
Sorption of water in melted PLA 98:2

T (K)	p ($\times 10^{-3}$ bar)	C (cm^3 (STP) cm^{-3})	C_a (cm^3 (STP) cm^{-3})
283.6	1.07	1.03	1.14
	1.08	1.18	1.30
	1.84	2.12	2.33
	2.63	2.67	2.94
	2.70	2.63	2.89
	4.07	3.93	4.32
	5.05	4.91	5.40
	6.57	6.22	6.84
	8.49	8.08	8.89
	10.07	9.90	10.89
293.0	1.48	1.00	1.10
	1.97	1.35	1.49
	5.18	3.45	3.79
	10.36	6.90	7.59
	14.66	9.91	10.90
	19.66	13.25	14.57
303.0	1.90	1.03	1.13
	3.95	1.59	1.75
	12.36	4.85	5.34
	19.79	7.88	8.67
	26.50	10.63	11.69
	32.32	12.93	14.22
	37.32	15.23	16.75
313.0	1.30	0.29	0.32
	7.35	1.81	1.99
	15.41	3.82	4.20
	23.92	5.76	6.33
	29.13	7.15	7.86
	34.49	8.55	9.40
	39.74	9.95	10.95
	44.07	11.46	12.61

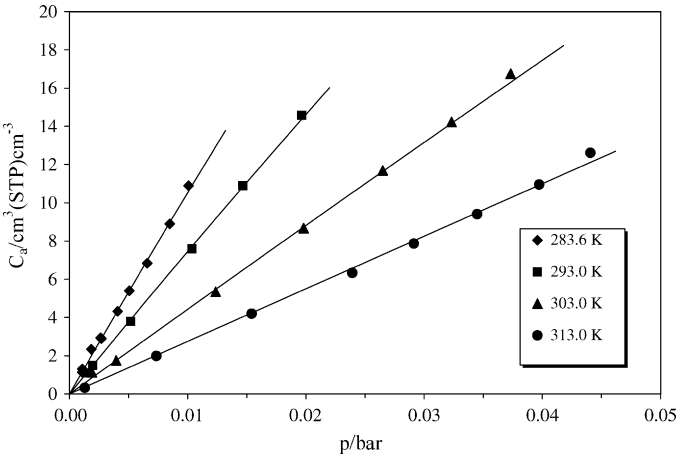

Fig. 5. Sorption isotherms of water vapor in melted PLA 98:2. Continuous lines represent the correlation with dual-mode sorption model.

any solute:

$$C_a = \frac{C}{\theta_a} \quad (5)$$

where C_a is the solubility in amorphous phase, C the experimental solubility of semi-crystalline polymer and θ_a is the amorphous volume fraction of the polymer [13]. Table 2 contains the adjusted parameters of the dual-mode sorption model and the absolute average deviations (AAD) for each gas and water vapor in melted PLA 98:2, for each isotherm.

Overall, it can be said that water vapor presents the highest solubility, followed by CO_2 and C_2H_4. This order is related to the condensability of the sorbates, as can be seen in Table 4 from the critical temperatures of the gases.

In order to address the effect of the thermal history of the PLA film in the gas/vapor solubility, sorption measurements were performed for the same sorbates in annealed PLA 98:2 between 283 and 313 K as a function of pressure, up to the atmospheric pressure and are the results are presented in Tables 6–8. In Figs. 6–8, the sorption results obtained for CO_2, water and ethylene, respectively, in annealed and melted PLA 98:2 at 303 K are compared. It can be concluded that the solubility for CO_2 and water in PLA films subjected to the two different thermal protocols is approximately the same, corroborating what was found in an earlier work for CO_2 at higher pressures (up to 50 bar) that the PLA 98:2 film thermal history does not significantly affect the magnitude of the gas sorption in this pressure an temperature range [6,7]. The results for the other studied temperatures indicate the same behaviour. However, in the ethylene case it can be seen that the solubility in annealed PLA is about 15% larger than in melted PLA at 303 K. An analysis of the dual-mode sorption model constants in Table 9 indicates that ethylene has predominantly a Langmuir type of sorption for both PLA thermal protocols, although the results obtained for the annealed PLA are smaller than the melted PLA. This analysis was done based on the relative magnitude of the term $C'_H b$ in Eq. (4). Since Langmuir type of sorption is intimately related to the presence of excess free volume, these results show that the annealed PLA should have larger free volume that the melted, which is the

Table 6
Sorption of carbon dioxide in annealed PLA 98:2

T (K)	p (bar)	C (cm^3 (STP) cm^{-3})	C_a (cm^3 (STP) cm^{-3})
284.1	0.158	0.76	0.95
	0.312	1.37	1.72
	0.492	2.00	2.50
	0.616	2.55	3.18
	0.815	3.34	4.18
	1.000	4.03	5.04
	1.098	4.45	5.56
293.9	0.121	0.47	0.59
	0.315	1.18	1.47
	0.721	2.51	3.14
	1.032	3.42	4.27
303.0	0.116	0.33	0.41
	0.256	0.72	0.90
	0.404	1.12	1.40
	0.592	1.60	2.00
	0.730	1.95	2.43
	0.869	2.29	2.86
	1.019	2.63	3.29
312.1	0.590	0.96	1.20
	0.715	1.06	1.33
	0.862	1.21	1.52
	1.023	1.40	1.75

Table 7
Sorption of ethylene in annealed PLA 98:2

T (K)	p (bar)	C (cm^3 (STP) cm^{-3})	C_a (cm^3 (STP) cm^{-3})
283.3	0.111	0.29	0.35
	0.257	0.71	0.85
	0.412	1.08	1.29
	0.562	1.39	1.66
	0.723	1.74	2.09
	0.931	2.11	2.54
	1.023	2.27	2.73
292.7	0.110	0.21	0.25
	0.214	0.42	0.51
	0.355	0.74	0.89
	0.549	1.07	1.28
	0.632	1.21	1.45
	0.796	1.49	1.79
	0.899	1.66	1.99
	1.023	1.84	2.21
302.6	0.106	0.17	0.21
	0.228	0.37	0.44
	0.355	0.56	0.67
	0.511	0.78	0.94
	0.657	1.00	1.20
	0.775	1.17	1.40
	0.918	1.36	1.63
	1.021	1.49	1.79
312.1	0.616	0.77	0.92
	0.695	0.90	1.08
	0.872	1.08	1.30
	1.029	1.25	1.50

Table 8
Sorption of water vapor in annealed PLA 98:2

T (K)	p ($\times 10^{-3}$ bar)	C (cm^3 (STP) cm^{-3})	C_a (cm^3 (STP) cm^{-3})
283.3	1.36	1.34	1.60
	2.70	2.50	2.99
	3.73	3.06	3.67
	4.53	3.56	4.27
	4.93	4.20	5.04
293.2	1.63	0.95	1.14
	6.32	4.26	5.11
	12.99	8.20	9.84
	14.09	8.60	10.32
303.1	6.46	2.83	3.39
	10.39	4.40	5.29
	15.06	5.23	6.28
	16.88	6.34	7.61
	23.79	8.59	10.30
	23.90	8.49	10.19
	26.64	9.55	11.46
313.1	3.23	0.75	0.90
	10.07	2.58	3.09
	10.12	2.65	3.19
	16.53	4.16	5.00
	23.64	5.43	6.52
	26.19	6.34	7.61
	28.78	6.25	7.50
	33.56	7.41	8.90

opposite of the expected, and can only be explained by the presence of large percentage of crystallites, which can act as virtual cross linkers and thus enhancing the available free volume. Note that this is a general discussion and does not give any information about the distribution of the free volume in the polymer film (Table 3).

In order to address the effect of the L:D content in the gas/vapor sorption, a comparison between annealed and melted PLA 98:2 and literature results for annealed PLA 80:20 [8] is provide in Figs. 6–8. Again, two different types of behaviour

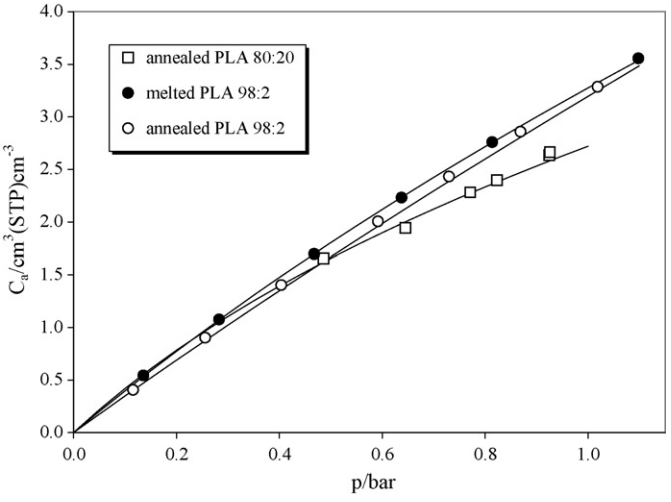

Fig. 6. Comparison of the solubility of carbon dioxide in annealed and melted PLA 98:2 with annealed PLA 80:20 [8] at 303 K. Continuous lines represent the correlation with dual-mode sorption model.

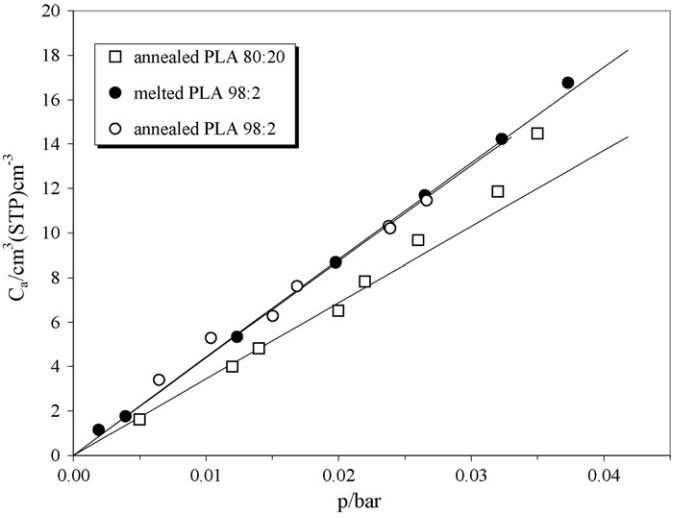

Fig. 7. Comparison of the solubility of water vapor in annealed and melted PLA 98:2 with annealed PLA 80:20 [8] at 303 K. Continuous lines represent the correlation with dual-mode sorption model.

are obtained: CO_2 and water vapor show the same behaviour, that is the solubility in PLA 80:20 is lower by 20% than the solubility in PLA 98:2, while ethylene has exactly the opposite behaviour, meaning that its solubility in PLA 80:20 annealed is larger by 20% than in PLA 98:2 annealed and by 40% in PLA melted. These results indicate that the L:D content has an important influence in gas solubility, probably due the difference in crystallinity and how it affects the available free volume.

An analysis of the dual-mode sorption model constants in Table 9 indicates that the Langmuir sorption mode is preferred by CO_2 and C_2H_4 in these low-pressure and temperature range. In a previous work, it was found that the sorption of CO_2 in the high-pressure region is Henry controlled [6]. This indicates that for this sorbate two distinct mechanisms occur depending on the pressure conditions: in the low pressure region, sorption is mainly a result of the process of filling free volume holes while in the high pressure region sorption is due dissolution in the

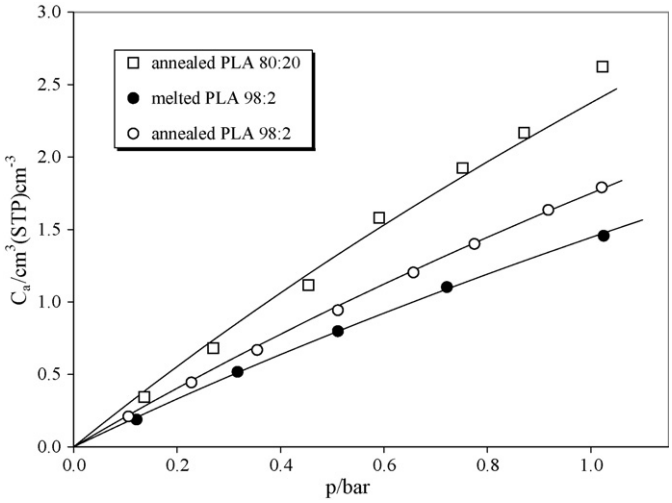

Fig. 8. Comparison of the solubility of ethylene in annealed and melted PLA 98:2. Continuous lines represent the correlation with dual-mode sorption model.

Table 9
Dual-mode sorption model parameters for carbon dioxide, ethylene and water vapor in PLA 98:2

T (K)	k_D (cm^3(STP) cm^{-3} bar^{-1})	C'_H (cm^3 (STP) cm^{-3})	b (bar^{-1})	$C'_H b$ (cm^3 (STP) cm^{-3} bar^{-1})	%Lang[a]	AAD%
CO_2 in melted PLA						
283.1	1.55	9.20	0.82	7.54	83	1.4
293.1	1.37	7.98	0.60	4.80	78	0.9
303.2	1.28	6.98	0.40	2.79	69	0.5
313.4	1.19	6.70	0.24	1.61	57	0.5
C_2H_4 in melted PLA						
283.0	0.39	7.90	0.29	2.29	85	3.1
294.3	0.35	7.15	0.25	1.79	84	3.7
303.2	0.32	5.85	0.24	1.39	81	2.6
313.1	0.30	5.40	0.23	1.24	81	2.4
H_2O in melted PLA						
283.6	670.00	50.00	8.30	415.00	38	3.8
292.9	497.00	39.60	6.70	265.32	35	1.7
302.9	362.00	25.90	3.24	83.92	19	4.7
312.9	265.00	12.80	0.80	10.24	4	3.2
C_2H_4 in annealed PLA						
283.3	0.66	7.30	0.39	2.85	81	1.9
292.7	0.58	6.20	0.34	2.11	78	3.4
302.6	0.55	5.20	0.30	1.56	74	2.2
312.1	0.52	4.30	0.28	1.20	70	1.3

[a] Lang (%) $= 100 \times C'_H b/(k_D + C'_H b)$.

polymer matrix. This duality is in fact the essence of the dual mode sorption model, which is well documented in the literature [11,13,14]. On the other hand, the water vapor solubility in PLA 98:2 is governed by Henry's law type of mechanism, which is an indication of the large amounts of water sorbed in the polymer even at low pressures.

As mentioned, C'_H represents the maximum amount of penetrant sorbed into the microvoids and can be an indication of the excess free volume of a glassy polymer. The magnitude of C'_H at a given temperature follows the condensability order, $H_2O > CO_2 > C_2H_4$. The data collected from the QCM allows the exploration of the temperature dependence of the dual-mode sorption model parameters. The apparent Langmuir capacity diminishes as the temperature approaches the glass transition temperature of the polymer, since the excess free volume tends to zero at that temperature. This observation is consistent with the results obtained, where the value of the product $C'_H b$ decreases with temperature, as it can be observed in Table 9.

5. Conclusions

The QCM technique was successfully used to measure the solubility of CO_2, C_2H_4, and water vapor in PLA with 98:2 (L:D) content, within the temperature range from 283 to 313 K and pressures up to 1 bar. In order to address the temperature conditioning effect in the gas polymer sorption, two different thermal treatments were used. It was observed that the sorption of CO_2 and water in PLA 98:2 in this temperature and pressure range is independent of the temperature protocol used, while ethylene shows a larger solubility in annealed than in melted PLA 98:2, which can be probably explained by the creation of extra free volume due to the presence of different percentage of crystallites. Also, CO_2 and ethylene sorption is governed by Langmuir type of mechanism, which is mainly a process of free volume filling, an entropic effect. In the case of water, the preferred sorption mechanism is the sorbates dissolution in the polymer matrix (Henry's law type of sorption), meaning that its sorption is conditioned by an enthalpic effect.

Also, comparisons with the CO_2 and water sorption in PLA 98:2 and PLA 80:20 show that their sorption is smaller in last one, while ethylene shows exactly the opposite behaviour. These facts indicate that the PLA thermal history influences the sorption of some sorbates, while the L:D content plays an important role in the sorption all of them.

Acknowledgments

This project was financed by Fundação para a Ciência e Tecnologia, POCTI/EQU/43356/2001. N.S. Oliveira thanks *Fundação para a Ciência e a Tecnologia* the Ph.D. scholarship (SFRH/BD/6690/2001).

References

[1] R. Auras, B. Harte, S. Selke, Macromol. Biosci. 4 (2004) 835–864.
[2] J.R. Dorgan, H. Lehermeier, M. Mang, J. Polym. Environ. 8 (1) (2000) 1–9.
[3] C. Zhang, J. Wyatt, S.P. Russel, D.H. Weinkauf, Polymer 45 (2004) 7655–7663.
[4] C. Zhang, J. Wyatt, D.H. Weinkauf, Polymer 45 (2004) 7665–7671.
[5] S.P. Russell, D.H. Weinkauf, Polymer 42 (2001) 2827–2836.
[6] N.S. Oliveira, J. Dorgan, J.A.P. Coutinho, A. Ferreira, J.L. Daridon, I.M. Marrucho, J. Polym. Sci.: Part B: Polym. Phys. 44 (2006) 1010–1019.
[7] N.S. Oliveira, J. Dorgan, J.A.P. Coutinho, A. Ferreira, J.L. Daridon, I.M. Marrucho, J. Polym. Sci.: Part B: Polym. Phys., in press.

[8] N.S. Oliveira, J. Oliveira, T. Gomes, A. Ferreira, J. Dorgan, I.M. Marrucho, Fluid Phase Equilibr. 222/223 (2004) 317–324.
[9] G. Sauerbrey, Z. Phys. 155 (1959) 206–222.
[10] V.M. Mecea, Sens. Actuators A 40 (1994) 1.
[11] S. Kanehashi, K.J. Nagai, Membr. Sci. 253 (2005) 117–138.
[12] H.J. Lechermeier, J.R. Dorgan, J.D. Way, J. Membr. Sci. 4922 (2001) 1.
[13] C.C. McDowell, Sorption and transport of acetone in random copolymers of poly(ethylene terephthalate) and poly(ethylene 2,6-naphthalate), PhD Thesis, North Carolina State University, USA, 1998.
[14] Y. Tsujita, Prog. Polym. Sci. 28 (2003) 1377–1401.
[15] Ely S J., F NIST Mixture Property Program (DDMIX), National Institute of Standard and Technology, 1990.